Railway track inspection and maintenance priorities due to dynamic coupling effects of dipped rails and differential track settlements

Kaewunruen, Sakdirat; Chiengson, Chatpong

DOI:
10.1016/j.engfailanal.2018.07.009

Document Version
Peer reviewed version

Citation for published version (Harvard):
Kaewunruen, S & Chiengson, C 2018, 'Railway track inspection and maintenance priorities due to dynamic coupling effects of dipped rails and differential track settlements', *Engineering Failure Analysis*, vol. 93, pp. 157-171. https://doi.org/10.1016/j.engfailanal.2018.07.009

Accepted Manuscript

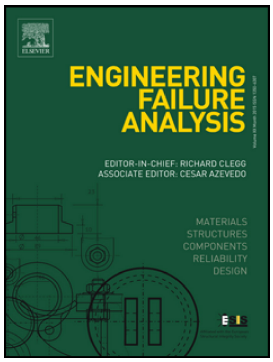

Railway track inspection and maintenance priorities due to dynamic coupling effects of dipped rails and differential track settlements

Sakdirat Kaewunruen, Chatpong Chiengson

PII:	S1350-6307(18)30326-1
DOI:	doi:10.1016/j.engfailanal.2018.07.009
Reference:	EFA 3539
To appear in:	*Engineering Failure Analysis*
Received date:	11 March 2018
Revised date:	5 July 2018
Accepted date:	5 July 2018

Please cite this article as: Sakdirat Kaewunruen, Chatpong Chiengson , Railway track inspection and maintenance priorities due to dynamic coupling effects of dipped rails and differential track settlements. Efa (2018), doi:10.1016/j.engfailanal.2018.07.009

Railway track inspection and maintenance priorities due to dynamic coupling effects of dipped rails and differential track settlements

Sakdirat Kaewunruen[a, b,*] s.kaewunruen@bham.ac.uk**, Chatpong Chiengson**[a]

[a]Birmingham Centre for Railway Research and Education, School of Engineering, The University of Birmingham, Birmingham B152TT UK

[b]TOFU Lab (Track engineering and Operations for Future Uncertainties), Department of Civil Engineering, The University of Birmingham, Birmingham B152TT UK

*Corresponding author.

Abstract

Each year, there can be three to six millions of service train axles running over an open plain track. In fact, these trains could impose a variety of dynamic loading conditions depending on the wheel and rail maintenance levels. Inevitably, the risk of high-intensity dynamic loading conditions by wheel-rail interactions due to wheel or rail irregularity cannot be disregarded. Imperfection of rail tracks could lead directly to the exceedance of permissible stress of a track component and later amplify rapid track deterioration rates causing cracking in sleepers and failure of track substructure. Practical railway track irregularities can be typically classified into short wave length (high frequency) and long wave length (low frequency) defects, of which previous researchers had studied each in isolation. This paper is the first to study the influence on railway track inspection and maintenance priorities caused by the coupling of wave lengths between dipped rail joint and differential track settlements. To study the dynamic coupling effects, P1 and P2 forces are evaluated at the track irregularity together with rail/sleeper contact force, ballast pressure and bending moments of sleepers using dynamic multi-body simulation approach. It is found that some patterns of coupling irregularity could cause a significant reduction in dynamic impact factors whilst some are associated with an increase in the wheel/rail impact force. The insight has then been integrated to establish track performance indicators that are paramount for prioritising track inspection and maintenance.

Keywords: rail joint, track irregularity, short wavelength defect, long wavelength defect, coupling track-vehicle interaction, track inspection, track maintenance

1. Introduction

Nowadays railways can be considered as one of the most efficient means of transportation, especially for the range of mobility between 100km to 1,000 km [1-3]. In the operation of railway lines, infrastructure managers have tried to minimise the maintenance expenditure while still keeping the track and vehicles in their state of acceptable conditions in accordance with the railway standards. In practice, the maintenance strategy and planning are empirically established to maintain the safety and efficiency of asset operations and maintenance, including safety-critical activities such as track inspections, maintenance schedule, emergency repair, operational restriction management, and other safety management. The goal of the empirical strategy (experience-based) is to minimise imminent failure of track structure and its components, and to reduce unplanned corrective maintenance costs, which are relatively expensive and time consuming. An imminent failure of any critical component at a specific location can cause further damage of infrastructure, giving risks of detrimental train derailments [4-6].

In general, the vehicle-track interaction force tends to change its form (e.g. increased magnitude, shorter duration, higher frequency) due to train speed and defect sizes [7-11]. Past studies have made efforts to understand the influence of short and long wavelengths separately [12, 13], while this study will evaluate the coupling dynamic vehicle-track interactions over coupled short and long wavelength rail defects, which aim at providing novel insights into the dynamic behavior of the vehicle-track system in different scenarios with D-track dynamic simulation program.

The detailed modelling of rail track dynamic and wheel-rail interaction was studied in 1992 while the D-track program for dynamic simulation was initially created by Cai at Queen's

University Canada [14]. Subsequently, Iwnicki set a benchmark, the Manchester Benchmarks in 1998 [15]. In 2005; Steffens [16] adopted the parameters of the Manchester Benchmarks to compare performance of various dynamic simulation programs and also developed the user-interface of D-track. On the other hand, the initial D-track still had an issue since its numerical results tended to be lower than others. Leong [17] had revised the program after this benchmark, and subsequently derived new Benchmark II with the revised version of D-Track in 2007. The updated results have been validated and the discrepancy is less than 15% [17]. D-Track (educational version) has been chosen in this study.

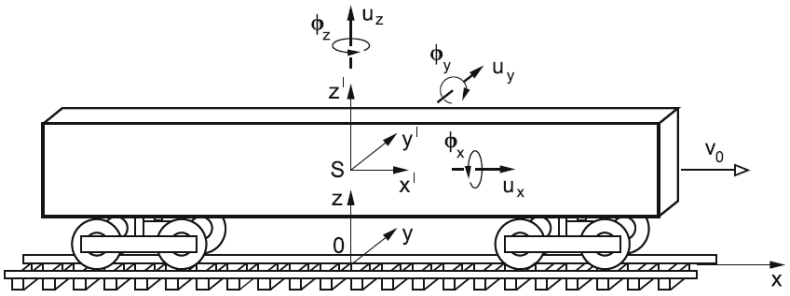

Fig. 1: Coupling vehicle-track model [16]

In this study, the dynamic multi-body simulation concept by Cai [14] has been adopted as seen in Fig. 1. The track model has included Timoshenko beam theory for rail and sleepers and Hertzian theory for the wheel-rail contact model, which enabled more accurate behaviour of tracks. This study is the first to establish multi-body simulations of coupling train-track interaction over coupled short and long wavelength defects (i.e. dipped rails and track settlement, respectively). Its aim is to establish a thorough criteria and guideline for prioritising track inspection and maintenance regimes, which has not been paid for special attention before [13]. The insight will help rail engineers improve safety and efficiency of rail infrastructure systems, underpinning both economic and environmental sustainability.

2. Dynamic load factor

To design railway tracks, each component need to be safely designed and meet systems requirements by various stakeholders. All track components are important for carrying the various types of load burdens from freight or passenger trains such as static and quasi-static loads, dynamic force and high-intensity impact force. There are a few design concepts, which are essential for appropriate analysis of the track components. These design concepts include permissible stress design (PSD) and limit states design (LSD) methods. A criterion in these design methods requires a dynamic impact factor. The dynamic impact factor is commonly defined by railway authorities in each country worldwide. It is usually based upon previous researches and field measurements of track forces and responses in representative rail lines [18].

In Australia, the most common method for calculation is presented by the Railway of Australia (ROA) manual also called "A Review of Track Design Procedures" or the "Blue Book" [18, 19]. The Dynamic Impact Factor (DIF) from this method ignores vertical track elasticity. The dynamic vertical wheel load (PD) is expressed empirically as a function of the static wheel load (Ps) where Ø is the Dynamic impact factor (always ≥ 1). For example, $P_D = \emptyset P_s$

The Eisenmann formula is the most common method used for calculation of the dynamic impact factor. At the same time, the Eisenmann formula is modified by ROA and is used in Australia and Europe [19]. The Eisenmann formula and modified Eisenmann are shown respectively below

$$P_D = (1 + \delta\eta t)P_s, \quad (1)$$

$$P_D = (1 + \delta\eta t\beta)P_s \quad (2)$$

where;

δ = Track condition factor

η = Speed factor, where $\eta = 1$for v < 60 km/hr and $\eta = 1 + \frac{v-60}{140}$ for v > 60 km/hr

t = Upper confidence level (UCL) factor

β = 1 for loaded vehicles; and 2 for unloaded vehicles.

Using this empirical method, track engineers can estimate the track forces acting on rail and other components such as fastening systems, sleepers, ballast and formation. This method is common and very useful in practice as field engineers and inspectors need to estimate the ability of components to withstand the track force.

3. Dipped rail joint

A dipped rail joint is a short-wavelength defect. A 'dipped angle' is a term used to define the sum of an angle of dipped trajectory between each rail and the horizontal (in milli-radians) at rail joints or welds. The two components of this angle consist of permanent deformation of the rail ends and the deflection of the joint under load as shown in Fig. 2 [20]. Jenkins et al. [21] state that the wheel travelling across a dipped rail joint creates the force peak as P1 and P2. The shape of the irregularity and characteristics of the vehicle create impact loading when the force at the dipped joint increases almost linearly with the speed and angle of the dip. When trains travelling

at high speed approach a rail joint, the wheel will lose contact with the railhead of rail and land on the connected rail which generates the high dynamic impact force as illustrated in Fig. 3.

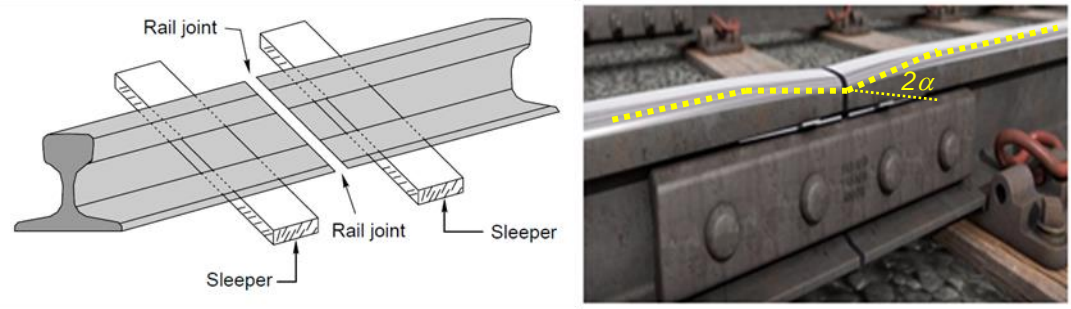

Fig. 2: Suspended rail joint [20]

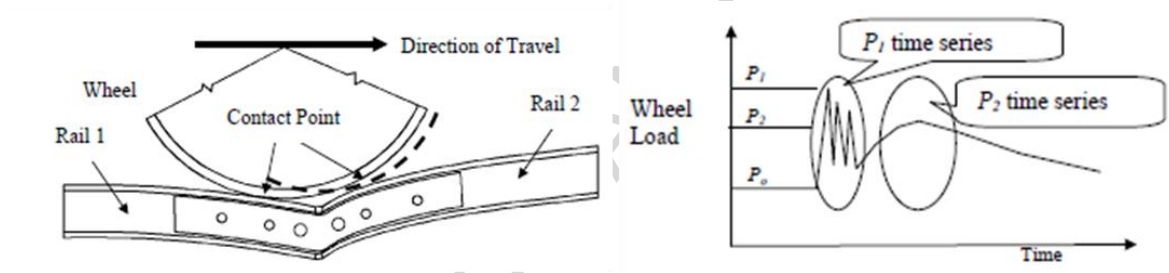

Fig. 3: Impact force of wheel/rail contact at dipped rail joint [13]

The P1 force is of a very high frequency (≅ 200 Hz to 1000Hz) and is less than 0.5 millisecond in length (0.25 - 0.5 millisecond after crossing the joint). The compression of contact zone between wheel and rail creates the inertia of rail and sleepers, which does not directly transform to ballast or subgrade settlement. However, it has a significant effect on wheel/rail contact force. The P2 occurs at a lower frequency range ((≅ 50 Hz to 200Hz) than P1 occurring much later at typically 6 – 8 milliseconds. The unsprung mass and the rail/sleeper mass are moving down together influencing the compression of the ballast below the sleeper. P2 forces therefore increase the contact stresses and also induce the loads on sleepers and ballast. P2 force

will be considered mostly by the track design engineer. Jenkins et al. [21] provided a method of calculation as follows:

$$P_1 = P_0 + (2\alpha v) \cdot \sqrt{\frac{k_H m_e}{1+m_e m_u}} \quad (3)$$

$$P_2 = P_0 + (2\alpha v) \cdot \sqrt{\frac{M_u}{M_u+M_t}} \left[1 - \frac{\pi C_t}{4\sqrt{K_t(M_u+M_t)}}\right] \times \sqrt{K_t M_u} \quad (4)$$

Where:

P_1 and P_2 = Dynamic rail force kN

P_0 = Vehicle static single wheel load kN

k_H = A chord stiffness to the Hertzian contact stiffness

m_e = The effective track mass kg

m_u = The vehicle unsprung mass kg

2α= Total joint angle rad

v = Speed of Vehicle m/s

K_t = Equivalent track stiffness MN/m

M_t = Equivalent track mass kg

C_t = Equivalent track damping kNs/m

4. Track settlement

Track settlement is a long-wavelength defect that can cause bumpy ride of the train passing. The train passing such the track settlement will induce higher dynamic load and increase high-frequency variations to the sleepers, ballast and subgrade. Increased dynamic loads will then cause non-elastic or plastic deformations with permanent setting of track foundation. In normal situations, the track will generally not return to the same position but to a very close point (accumulated deformation). As time passes, all non-elastic deformations will create a new track position and this phenomenon becomes differential track settlement. The track alignment and surface level of track also change due to the accumulated non-elastic deformations. The irregularity of the track will increase low-frequency oscillation of vehicles. However, the track settlement often takes place at the transition area to a bridge. In addition, the quality of ballast, sub-ballast and the subgrade are also factors inducing permanent deformation [22].

Track settlements typically consist of two phases. The first phase is after tamping when the gap between ballast particles is reduced quickly and so this layer is consolidated. The second phase is slower since the densification and inelastic behaviour of the ballast and subgrade materials are the main concern. The major parameters influencing the ballast settlement are the deviatoric stress, vibrations, degradation and subgrade stiffness. The empirical settlement equation for the substructure is shown below. This only considers the ballast settlement not including subgrade settlement [13]:

$$Z_{\mathrm{iN}} = Z_{i0} + f\left(\log N, \sigma_{\mathrm{be}}, I_{\mathrm{dyn}}, I_{\mathrm{dec}}, I_{\mathrm{Esub}}\right) \qquad (5)$$

This equation describes the settlement of ballast below the sleeper I where;

Z_{i0} = The given void amplitude

N = Number of load cycles

σ_{be} = The vertical equivalent stress in the ballast layer

I_{dyn}= The dynamic factor

I_{dec} = The degradation factor

I_{Esub} = The subgrade stiffness factor.

5. COUPLING VEHICLE-TRACK MODELLING

The vehicle-track model (using D-Track) is simulated by the Winkler foundation principle with a cross-section of track dynamic responses considered symmetrically. Rail and sleepers were represented as an elastic beam using the Timoshenko model. The sleepers provide support to the rails as discrete rigid supports. A free-body diagram of the track model is shown in Fig. 4(a) where *P(t)* is a moving wheel force at constant speed (v). Fig. 4 (b) represents the force from rail to sleeper through the rail seat (i^{th}) and reaction force $k_s z_i(y,t)$ per unit length.

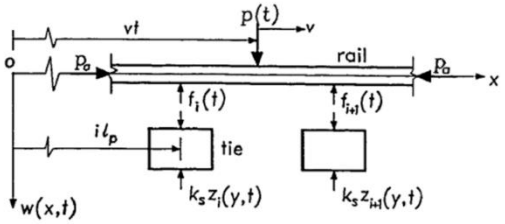

a) forces on the rail

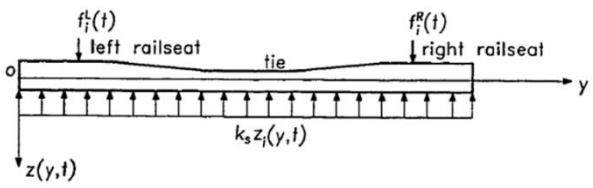

b) force on the sleeper

Fig. 4: Free-body diagram of track model [14]

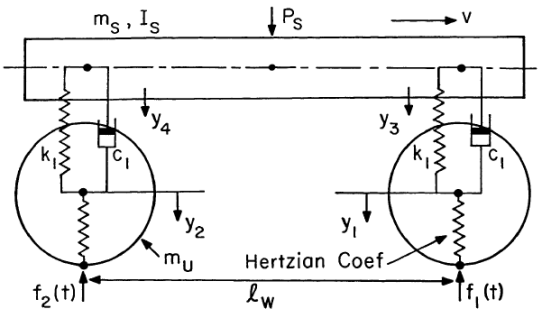

a) wheelset model

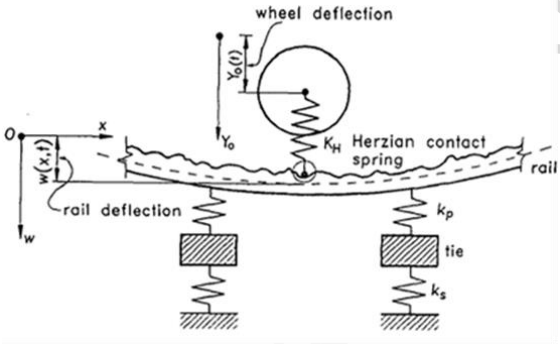

b) Herzian wheel-rail contact

Fig. 5: Free-body diagram of vehicle-track model [14]

The wheelset model in this study consists of multi degrees of freedom, which include one bogie with two-axles, rail and track. The wheelset model uses the unsprung masses (m_u) and the sideframe mass (m_s, I_s) to connect to the rails through the primary suspension (k_1, c_1) as shown in Fig. 5 (a). The components of vehicles are demonstrated as a spring load by using the Hertzian contact model. Moreover, the equations of motion in this model used the principles of Newton's law and structural beam vibrations. The integration between the wheelset and track equations can be calculated by the non-linear Hertzian wheel-rail interaction model as illustrated in Fig 5 (b). The D-Track model has been benchmarked by previous studies [18, 23-25] in order to assess the accuracy and verify the precision of numerical results. D-Track is thus adopted for this study.

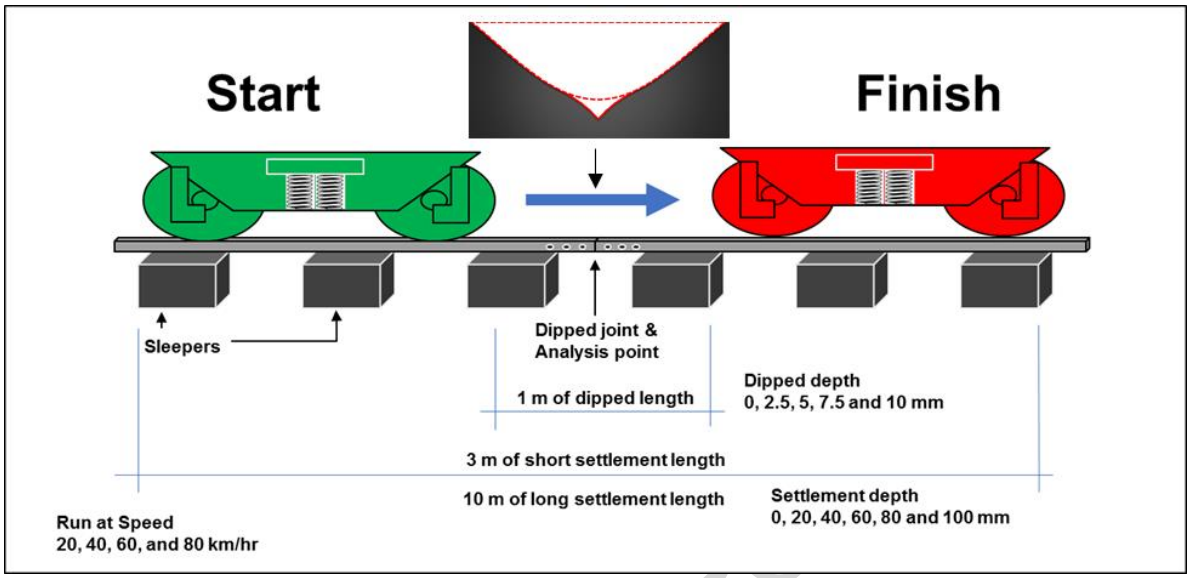

Fig. 6: Model of analysis position for coupled effects

As part of the analysis, the centre of irregularity including position of rail and sleeper are required. The dipped rail joint is fixed at midspan before the sleeper as an analysis position as shown in Fig 6. This paper is aimed at highlighting the result of the coupled dynamic effect at dipped rail joint of 0, 2.5, 5, 7.5 mm in depth and 10 mm with the settlement of 0, 20, 40, 60, 80 and 100 mm in depth (sleeper spacing is 600 mm). Short settlement (3m) and long settlement (10m) are assumed, following previous literature reviews of track settlement modelling [26-28] as presented in the example in Fig 7. The position of the sleeper analysis is at the rail seat and midspan of the sleeper. The DTRACK recommended a time step of 0.02 milliseconds then the model will report data for every fifth-time step.

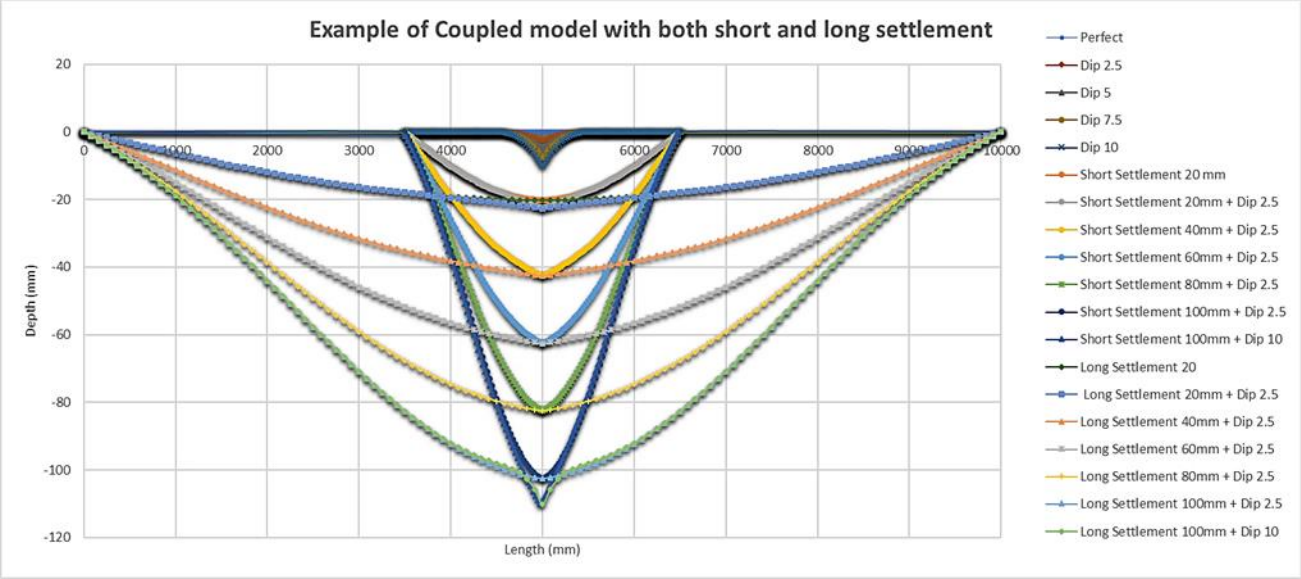

Fig. 7: Example of coupled model with both short and long settlements

Overall, there were 440 simulations carried out. The simulations include 55 models for the simulations for short settlement, 30 models for perfect track and long settlement, and 25 models without settlement at 0mm. These 110 models were further varied by four levels of speed that are simulated - 20, 40, 60 and 80 km/hr - with two analysis points on the sleeper (at mid span and rail seat). 106t freight wagon (260 kN of axle load) with wheel radius of 0.46m and Hertzian spring constant of 0.87×10^{11} N/m$^{3/2}$ running on the ballast track with concrete sleepers are used for the simulations.

6. Results and discussion

6.1. Wheel/rail contact force

The normal contact force between the wheel and rail is the first result considered at dipped rail joint with P1 and P2 forces in dipped rail joint area. P1 and P2 will be calculated in terms of DIF to evaluate the results. The dynamic impact force between wheel and rail on short settlement

coupling with dip of 10mm is shown in Fig. 8 while the long settlement with 10mm of dip is shown in Fig. 9 where: S is a short settlement, L is a long settlement first digit is the depth of settlement (mm) and the last digit is the depth of dipped rail joint (mm).

Fig. 8 presents the coupled effect of wheel/rail contact in short settlement. The perfect track is shown as a linear line at 1.02 of DIF while Eisenmann's equation is calculated to compare these results. It is found that the force increases when speed increases from 0 to 60 km/hr. However, the coupled effect shows the anti-resonant reduction of impact force because of wheel angle and wheel speed. On the other hand, at speed 80 km/hr, the coupled effect between short settlement and dipped rails of 10 mm (S 100 10) induces the maximum impact force (6.438 of DIF) because the wheel momentarily loses contact longer than only dipped rail (S 0 10) at the same speed and it thus creates higher contact force.

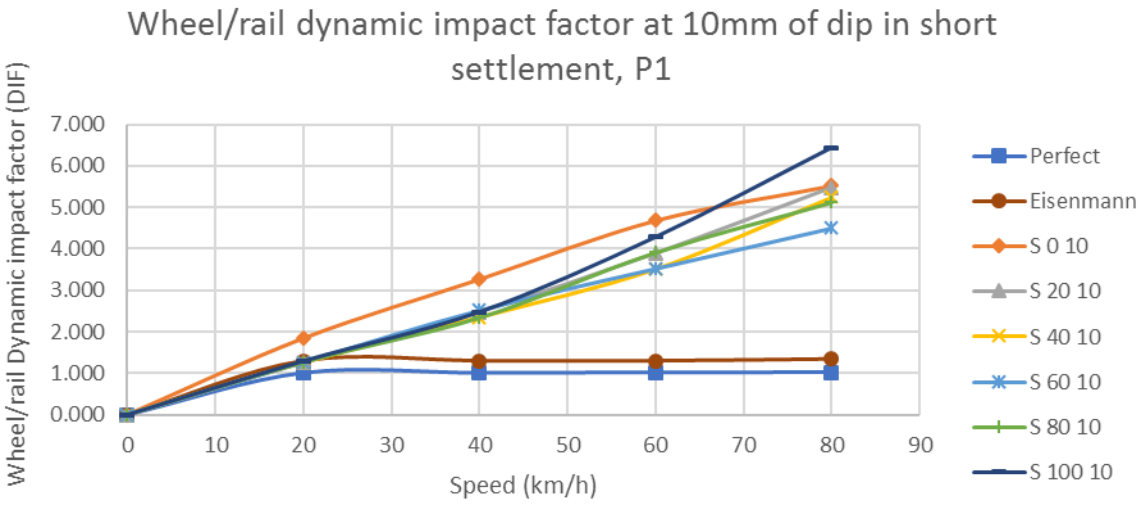

Fig. 8: Wheel/rail Dynamic impact factor at 10mm of dip in short settlement

Fig. 9 presents the DIF of P1 in a long track settlement. At low speed (0 - 40 km/hr), only a dipped rail joint of 10 mm (L 0 10) presents the highest impact loading whilst the other cases show somewhat a similar value. Surprisingly, an interesting effect can be observed for the

combined effect between 100 mm of track settlement and dipped rails of 10 mm or “L 100 10” as the curvilinear line happened at a speed of 60 km/hr, which shows the reduction in impact force.

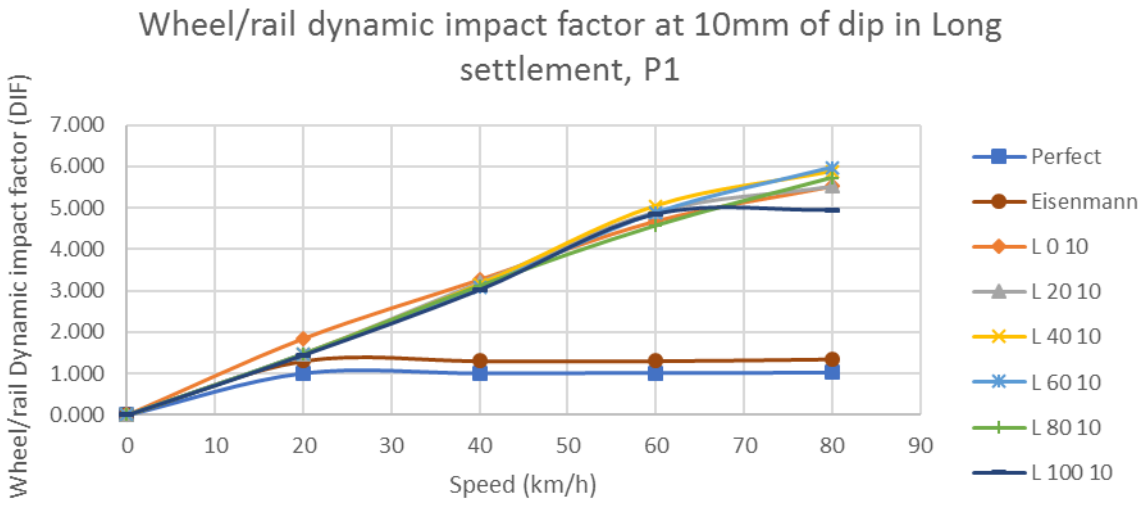

Fig. 9: Wheel/rail Dynamic impact factor at 10mm of dip in long settlement

Fig. 10 presents P2 wheel/rail contact forces. It is found that the peak value for the case of dipped rail joint (S 0 10) is at the speed of 20 km/hr, and its P2 reduces when train speeds increase. At 60 km/hr, the coupled effect creates a significant reduction in DIF after increasing at 80 km/hr with the maximum of 1.785 of DIF at “S 100 10”. Between 60 and 80 km/hr, the impact force increases with the settlement increase. From these results, it can be assumed that 60 km/hr may be the proper speed of safe operation for most wagon and track components located in the vicinity of the contact zone. Moreover, the calculated Eisenmann equation is higher than the simulation, at approximately 30%.

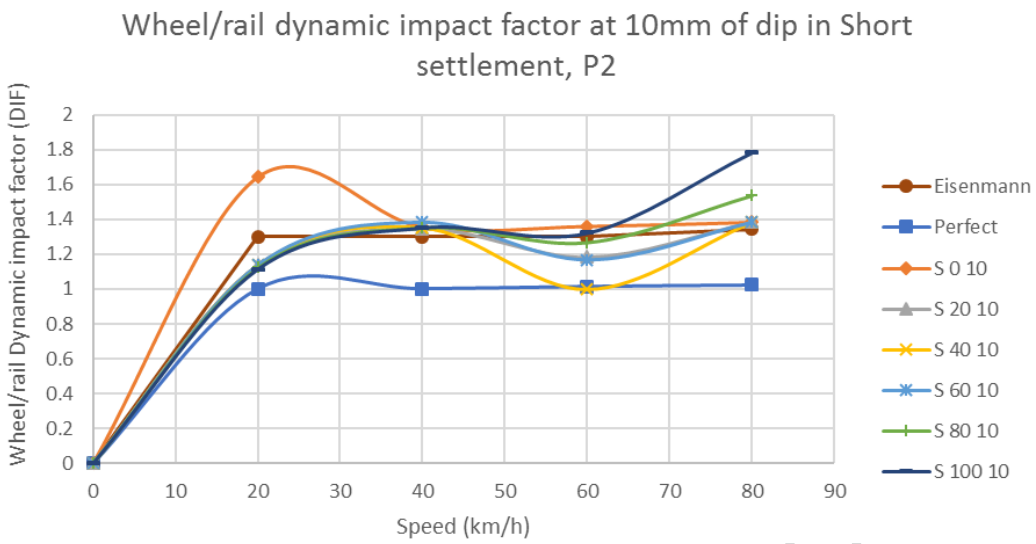

Fig. 10: Wheel/rail Dynamic impact factor at 10mm of dip in short settlement, P2

P2 forces are simulated in coupled long settlement as shown in Fig. 11. At low speed range, it is clear that the maximum impact force of P2 for the case of dipped rail joint (L 0 10) can be observed at 20 km/hr ("L 0 10" or only dipped rail joint). In contrast, other cases exhibit consistent impact force of P2 across the train speed range.

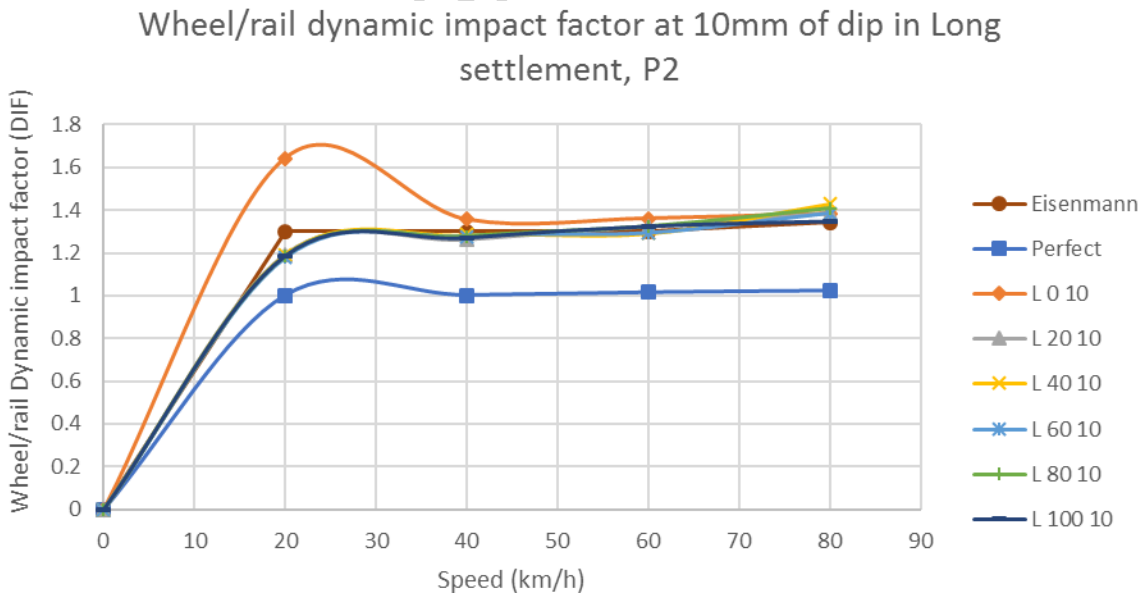

Fig. 11: Wheel/rail Dynamic impact factor at 10mm of dip in long settlement, P2

When considering the time domain frequency of coupling between settlement (short and long) of 100 mm and dip of 5 mm at 80 km/h, the result of coupled short settlement shows little reduction force (-10%) of P1 in a coupled effect as shown in Fig. 12 whilst P2 is increased, +25% when it is in the couple mode (S 100 5). On the other hand, when coupling with higher dipped rails at 10 mm, P1 and P2 forces will be increased significantly (+14%) as shown in Fig. 13.

In terms of coupled effect in long settlement, it creates a huge reduction in P1 of approximately -40% including decreases of P2, -25% when couple with dip of 5 mm and settlement of 100 mm (L 100 5) as shown in Fig 14. Once coupled with high dipped rail joint at 10 mm (L 100 10), P1 is still reduced slightly (-10%) and P2 is still the same as illustrated in Fig 15.

In conclusion, P1 force is able to be decreased when coupling between low dipped rails and small short settlement but will be increased once there is a high settlement and high dipped rail joints. These levels of load burdens should be avoided (by prioritizing track maintenance). Table 1 presents the comparison of the DIF: red highlight is increases and green highlight is decreases once considered in coupled mode.

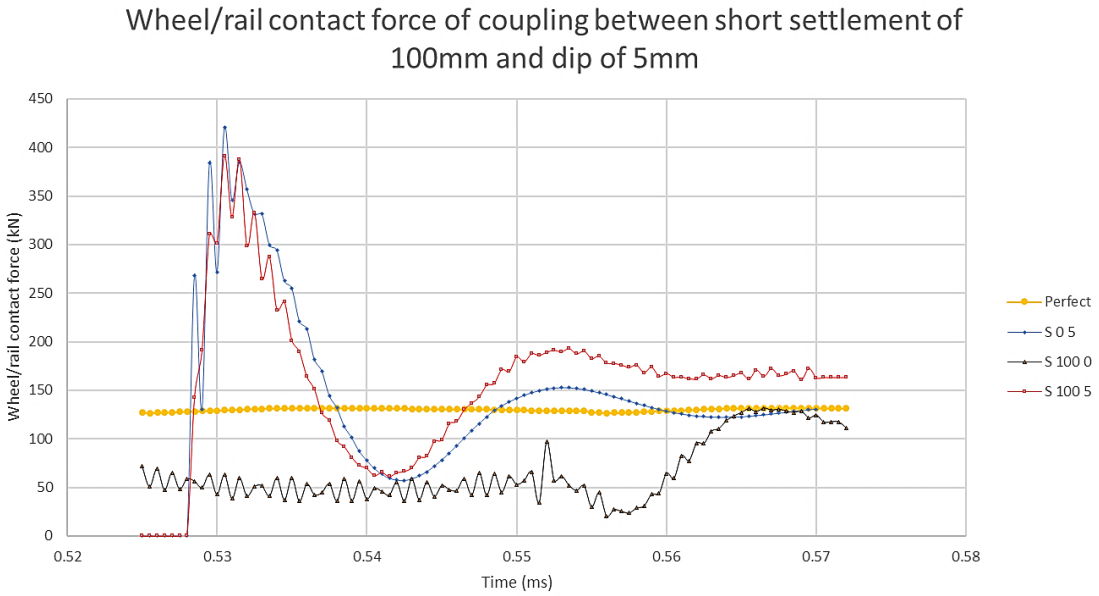

Fig. 12: Wheel/rail contact force of coupling between short settlement of 100mm and dip of 5mm

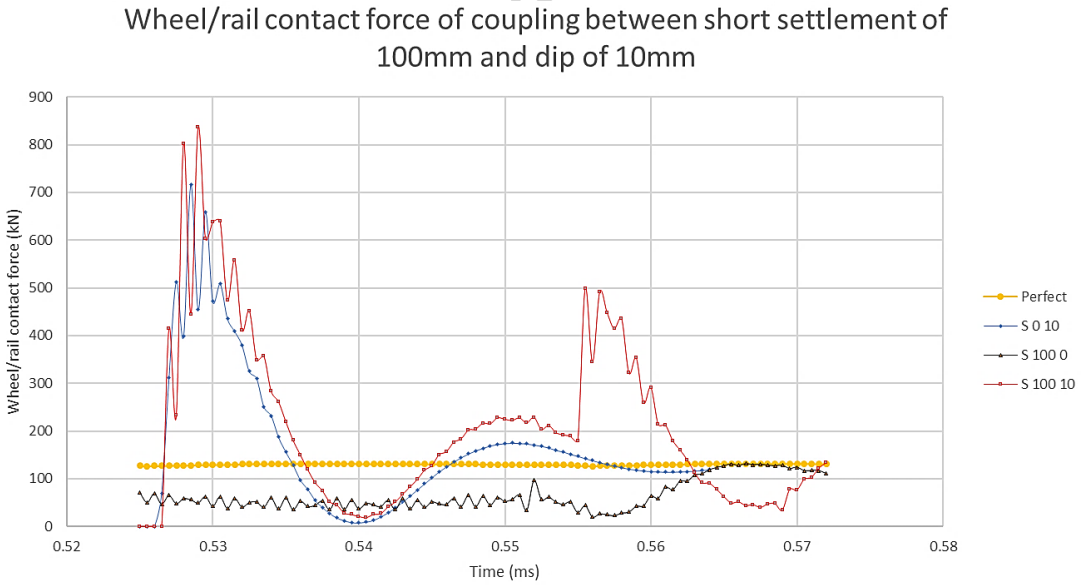

Fig. 13: Wheel/rail contact force of coupling between short settlement of 100mm and dip of 10mm

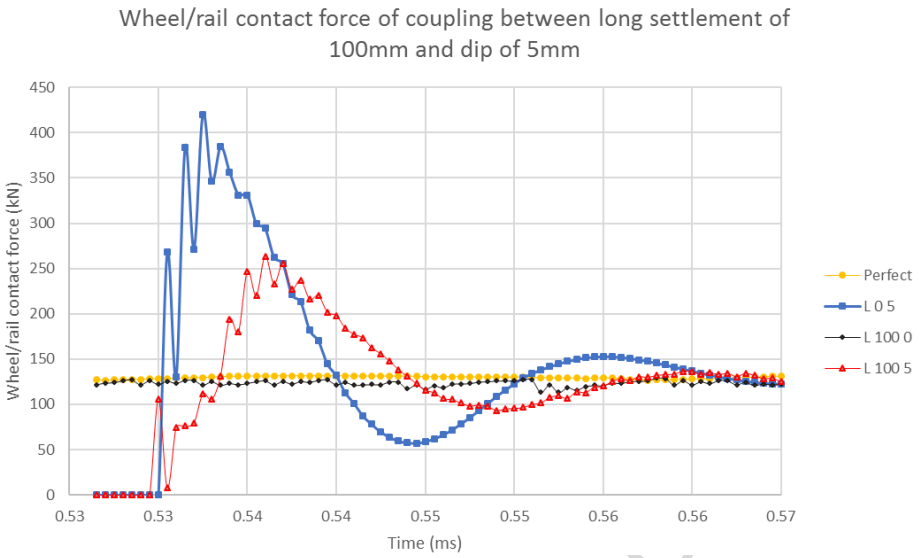

Fig. 14: Wheel/rail contact force of coupling between long settlement of 100mm and dip of 5mm

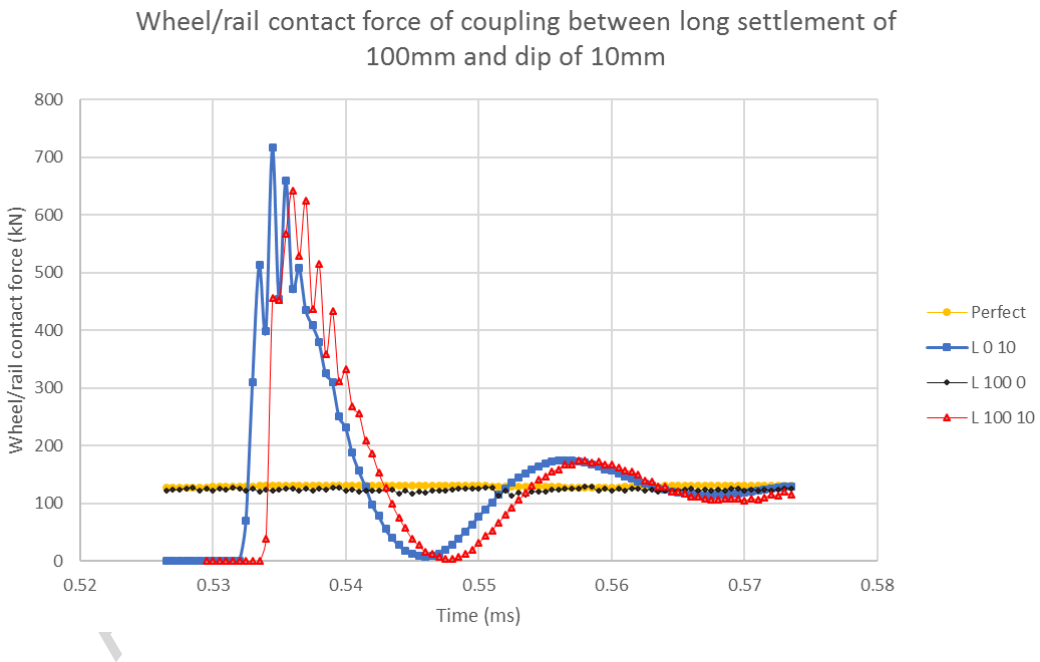

Fig. 15: Wheel/rail contact force of coupling between long settlement of 100mm and dip of 10mm

Table 1: The maximum DIF of P1 and P2 at speed of 80 km/hr in coupling mode of both short and long settlement

Type	Settle (mm) / Dip (mm)	Short settlement						Long settlement					
		0	20	40	60	80	100	0	20	40	60	80	100
P1	0	1.02	1.05	1.08	1.05	1.08	1.04	1.02	1.03	1.02	1.02	1.03	1.02
	2.5	1.88	1.42	1.47	1.48	1.62	1.17	1.88	1.62	1.58	1.58	1.57	1.55
	5	3.24	2.43	2.63	2.18	2.54	2.99	3.24	2.81	3.10	3.12	2.98	2.02
	7.5	3.98	3.92	3.90	4.15	4.29	5.04	3.98	4.57	4.55	4.05	4.71	4.61
	10	5.52	5.48	5.25	4.50	5.12	6.44	5.52	5.52	5.88	5.98	5.72	4.95
P2	0	1.02	1.05	1.08	1.05	1.08	1.04	1.02	1.03	1.02	1.02	1.03	1.02
	2.5	1.09	1.01	1.03	1.02	0.92	1.23	1.09	1.05	1.04	1.04	1.03	1.03
	5	1.22	1.06	1.02	1.15	1.31	1.53	1.22	1.24	1.19	1.19	1.17	1.05
	7.5	1.28	1.25	1.28	1.35	1.44	1.66	1.28	1.33	1.32	1.31	1.27	1.31
	10	1.39	1.39	1.39	1.39	1.54	1.79	1.39	1.39	1.43	1.39	1.41	1.35

6.2.Rail/sleeper contact force

The analysis of impact force at the contact between rail and sleeper are considered as shown in Figs. 16-19. Both P1 and P2 rail/sleeper force are decreased in the dipped joint zone when combining settlements with the dipped rail joint. The results show that the dipped rail joint has less impact on the coupling effect while the high impact forces happen when the wheel reaches

the settlement as shown in Fig. 16 and 17 for short and long settlement respectively. Moreover, P1 of rail/sleeper impact force increases when the settlement level increases. However, the dip level increases cannot significantly affect the rail/sleeper contact force as shown in Fig. 18. Considering P2 forces as shown in Fig. 19, DIF increases with size of short settlements. It is clear that the coupled effect between short settlement of 40mm and the dipped rails of 10mm (S 40 10) is pronounced due to the resonant frequency whilst the coupled effect does not influence the DIF in the cases of long settlement.

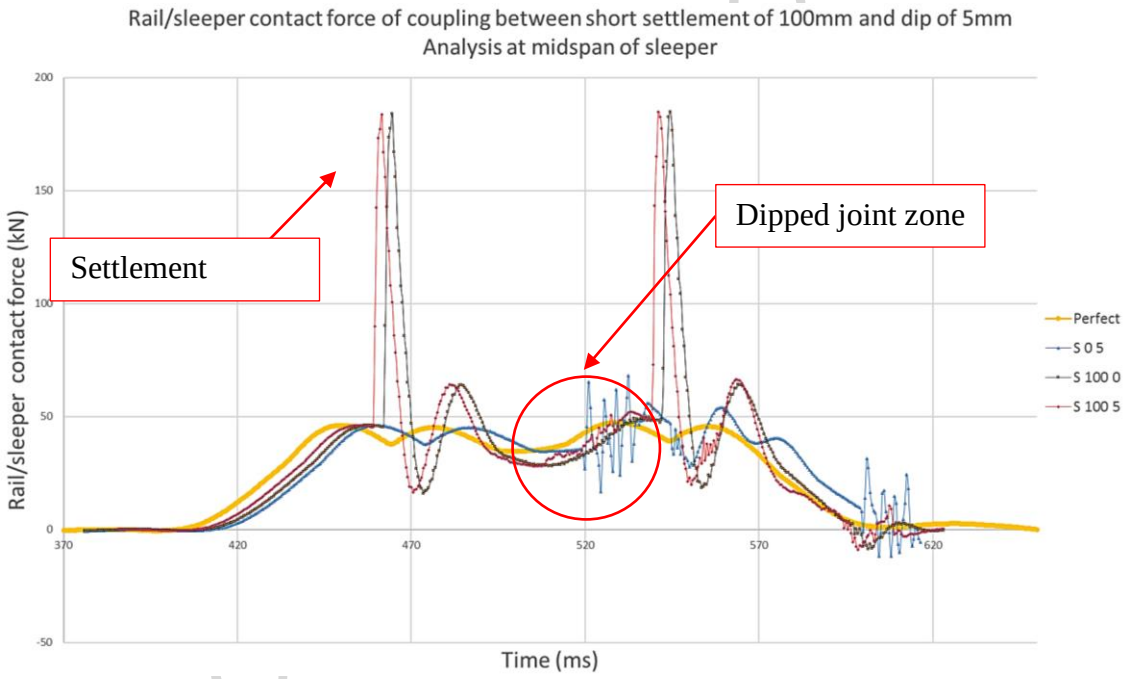

Fig. 16: Rail/sleeper contact force for short settlement at 80 km/hr with 260 kN of axle load

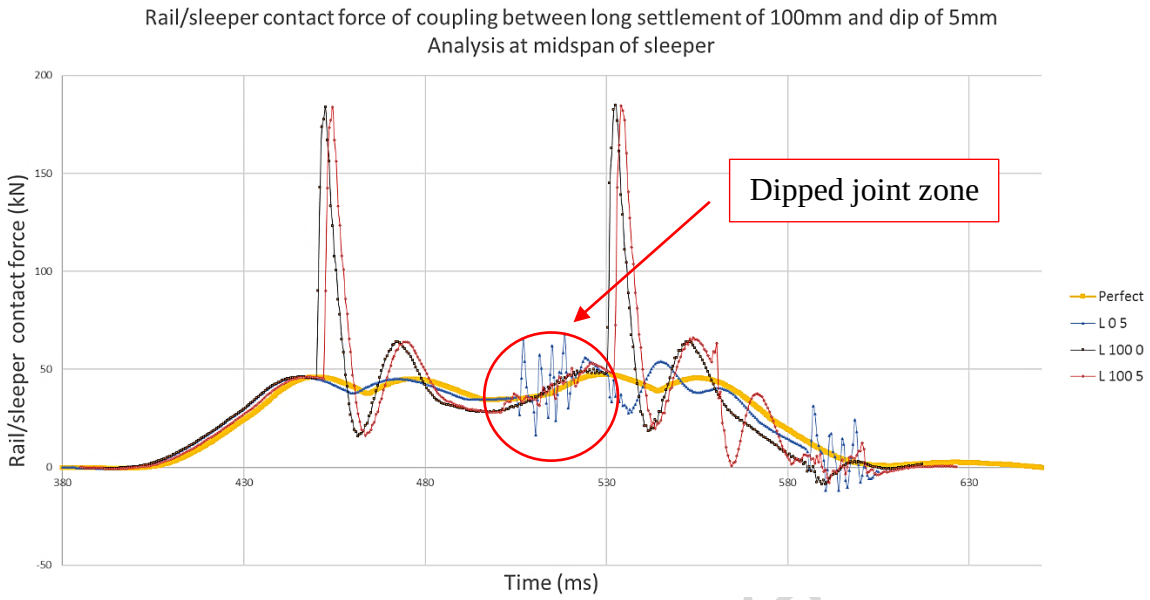

Fig. 17: Rail/sleeper contact force for long settlement at 80 km/hr with 260 kN of axle load

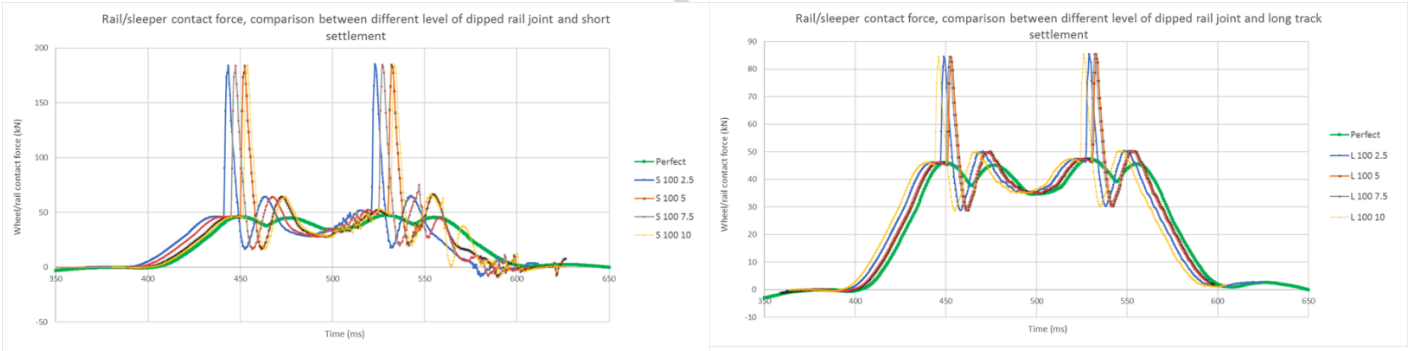

Fig. 18: Rail/sleeper contact force for short and long settlement at 80 km/hr with 260 kN of axle load

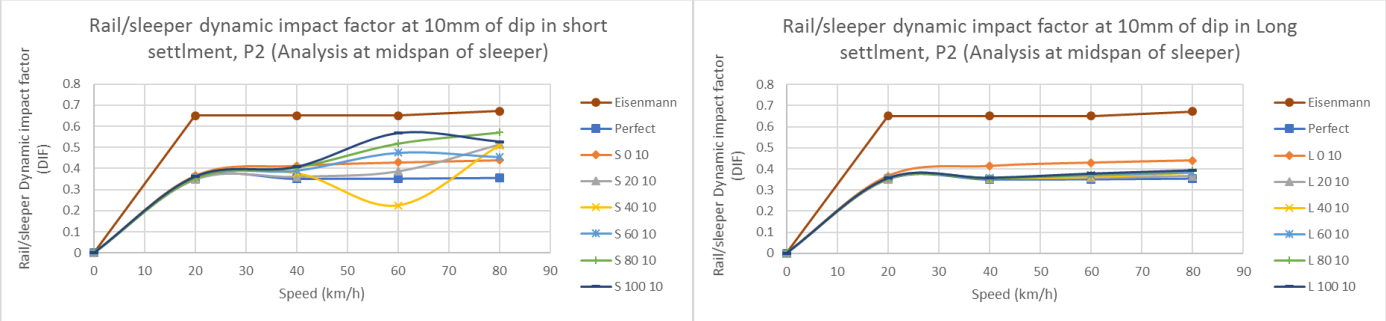

Fig. 19: P2 of rail/sleeper dynamic impact factor for short and long settlement at dip of 10mm

6.3.Ballast pressure

Maximum ballast pressures can be determined right underneath the sleeper. When the settlement increases, the ballast pressure can still be increased but the dipped rail joint coupled with tangential long wavelength defects cannot influence the ballast pressure. The peak pressure in the coupling of short settlement of 100 mm and dipped rails of 10 mm (S 100 10) is 850 kPa as shown in Fig. 20 and 21. The interesting point is the coupling "S 40 10" since the results calculated from rail/sleeper force, sleeper/ballast force, and ballast pressure show curvilinear phenomenon. Other results tend to be linear lines due to the effect of different levels of settlements along with coupled long settlements.

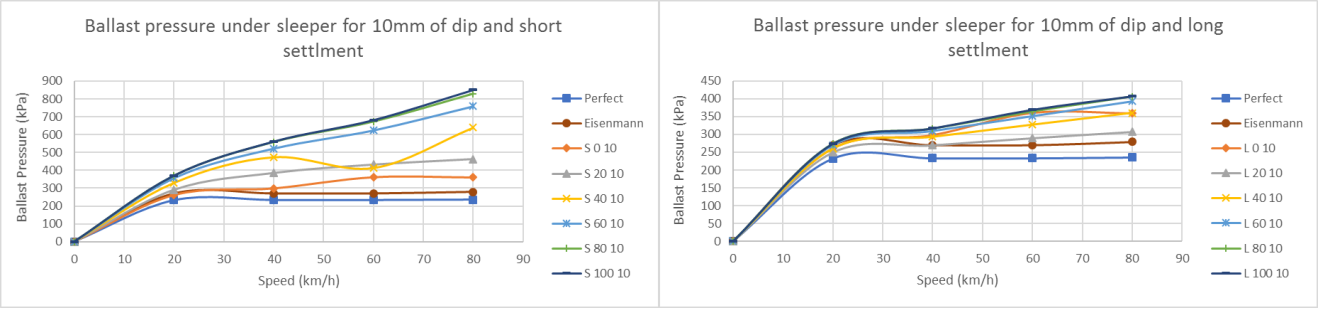

Fig. 20: Ballast pressure under sleeper of coupling between dip of 10mm and both short and long settlements with axle load of 260 kN

Dipped rail joints induce little effect on ballast pressure when combined with track settlements. A significant reduction of ballast pressure at dipped zone occurs on the coupled model “S 100 5” while only dipped rail joint (S 0 5) creates a high pressure at this zone, which is the same effect as the coupled long settlement as displayed in Fig.21.

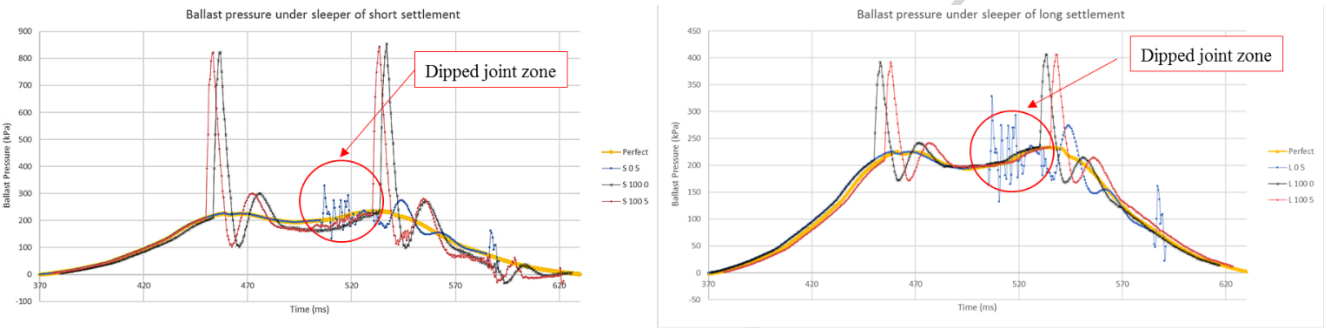

Fig. 21: Ballast pressure under sleeper of short and long settlements at 80 km/hr with axle load of 260 kN

6.4. Bending moment of rail at mid span before sleeper C

The bending moment of rail is analyzed at mid span of rail between sleepers before sleeper C (or the sleeper at the centre of track model) as the leading wheel experiences impact loads from the coupling between the dipped joint and track settlement. The length of sleeper is 2.6 m with standard gauge (1.435m). The trend in the graph shows that the bending moment increases as track degradation increases. It is apparent that “S 40 10” is still the uncommon condition because of remarkable rail seat load. The contrasting settlement in combine long settlement model is enhanced slightly to the coupling model. The surprising condition is a dipped joint of 10 mm (L 0 10). In this condition, an abnormal rise caused by resonant frequencies can be observed in Fig. 22. The coupled track settlement is also the key parameter to increase bending moment of rail

and the various degrees of dipped rail joint combined with track settlement, which cannot affect the bending moment of rail whether in short or long settlement as shown in Fig. 23 and 24.

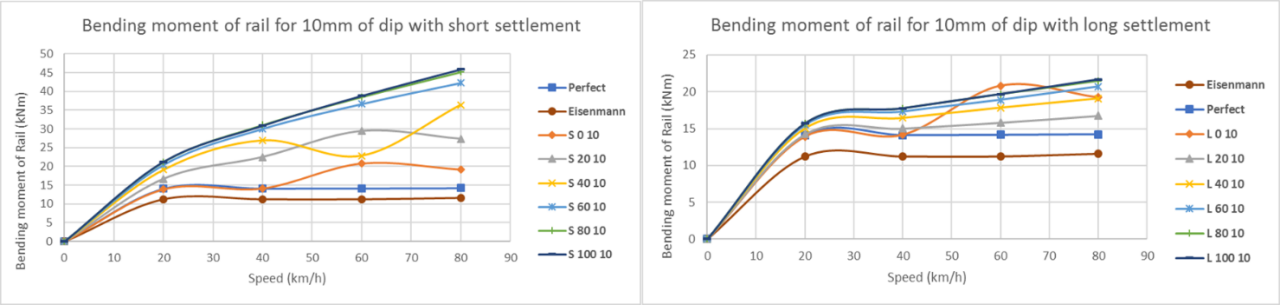

Fig. 22: Bending moment of rail for 10mm of dip with short and long settlement at 80 km/hr with axle load of 260 kN

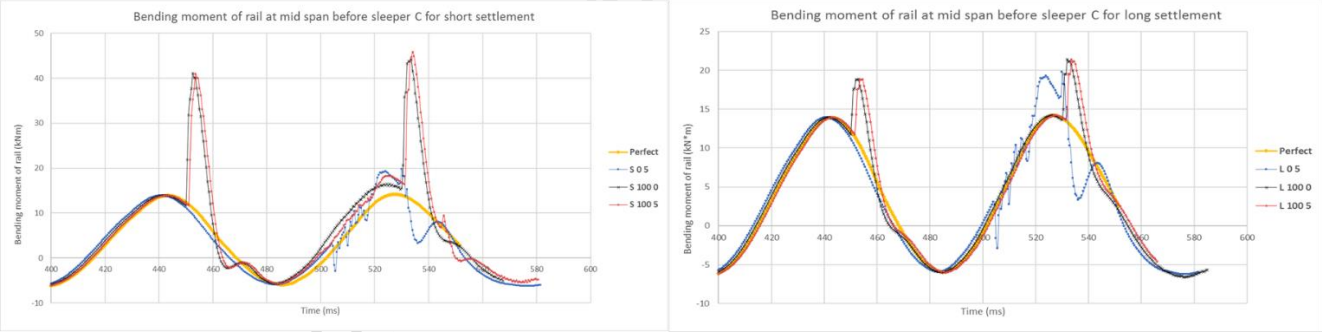

Fig. 23: Bending moment of rail at mid span before sleeper for short and long settlements

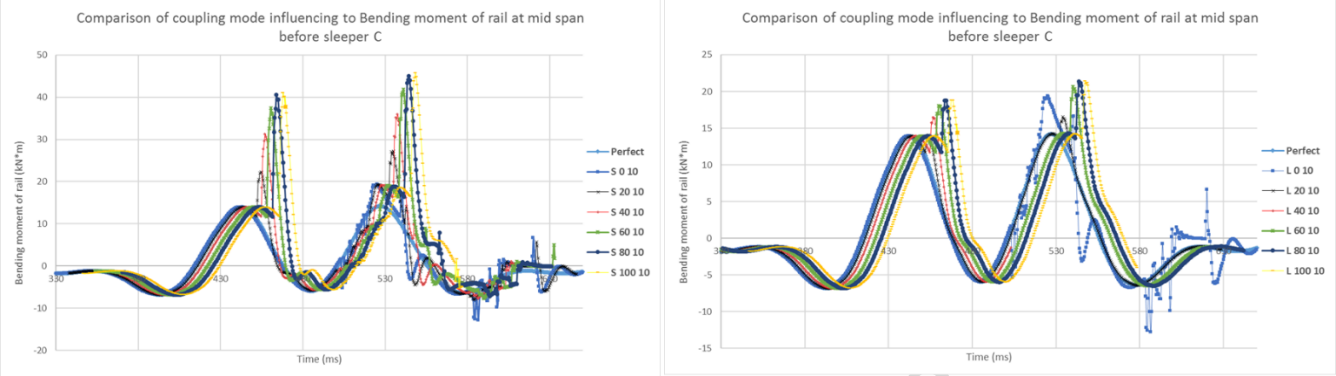

Fig. 24: Comparison of different levels of short and long settlemensts with 10 mm of dipped joint

7. Establishing performance indicators

To establish performance indicators for prioritizing track inspection and maintenance planning, an analysis of all the numerical results presented above is conducted and the following aspects will be used to draw the guidelines for practical railway implementation. It is important to note that:

- P1 force is specified in AS1085.14-2003 [29] as the lower limit of DIF is 2.5 times static wheel load which can potentially damage the local contact region of the wheel tread and rail head.
- P2 force in AS 7508:2017 [30] is typically limited at 230 kN for any rolling stock. The offload threshold was associated with increasing risk of track component failure along with damaged wagons.
- AS2758.7 [31] shows the ballast pressure should not exceed 750 kPa for high-quality ballast.

- The calculated maximum negative bending moment (at midspan) is 11 kNm while the maximum positive bending moment (at rail seat) is 23 kNm [32-40].

In coupled model of short settlement (3 m of length), the increasing rail deterioration rates can be expected due to high P1 force, particularly amplitudes of dipped rail greater than 3.75 mm with the entire range of track settlement.

Rapidly increasing track deterioration rates are forecasted with the amplitude of settlement greater than 70 mm with dipped rails higher than 2.5 mm. The beneath ballast performance deteriorates with the amplitude of track settlement, namely for settlement higher than 50 mm as shown in Fig. 25. In coupled short settlement, the higher risk of cracks at the rail seat can be assumed by using the maximum negative bending moment, which will appear with the amplitude of settlement higher than about 20 mm. It is expected that crack at midspan rates will be increased at the depth defect of settlement higher than 28 mm approximately shown in Figure 26.

Rail deterioration increases with the higher wheel/rail contact force and high P1 force was found in the couple model of long settlement, particularly with amplitudes of dipped rails more than 3.75 mm as shown in Fig. 27. It should be noted that in cases of bending moment failures of the sleepers and other components, these coupling dynamic interaction effects do not exceed the threshold value therefore it is not within the scope of this study. These insights can be correlated with in-service track behaviors, as evidenced in [39-41]. It has been reported that the track components deteriorate quickly, especially when there is a presence of water (e.g. mud pumping). This study has identified the effect of a short-wavelength defect coupled with track settlement. If there are more than one short-wavelength defects, such dynamic effect would likely to increase. This track problem can be observed in area with multiple joints/welds such as

switches and crossings, rail bridge ends, and the area for rail stress management (e.g. rail cut-in cut-out to manage elevated temperature stress) [42].

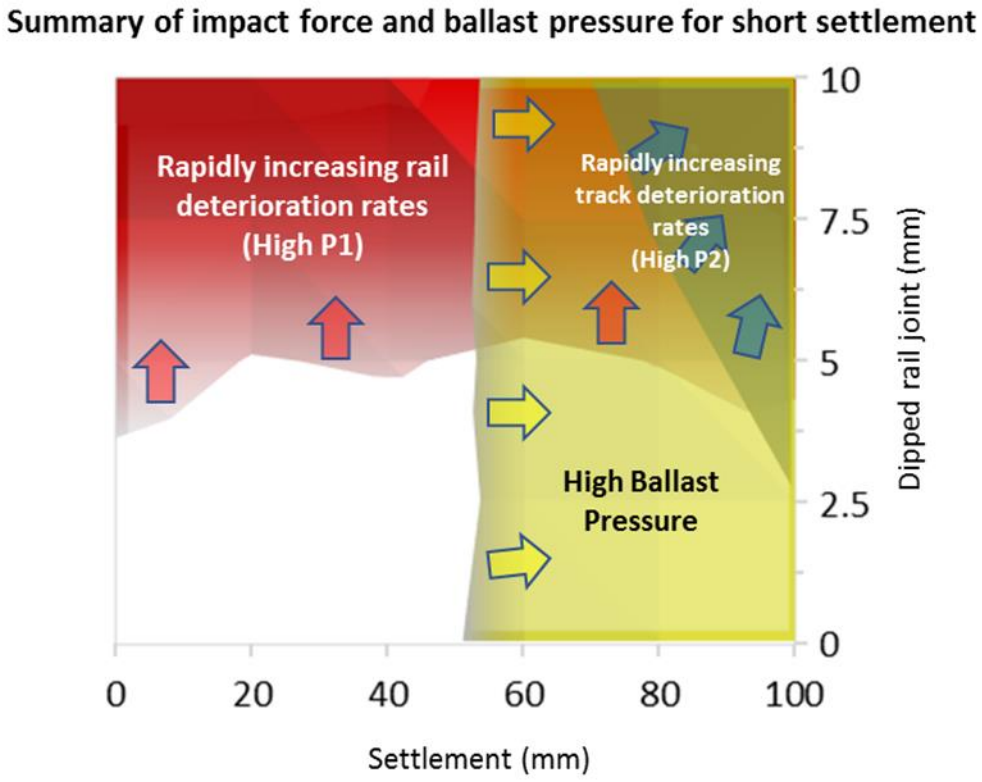

Fig. 25: Summary of wheel/rail interaction force and ballast pressure for short settlement

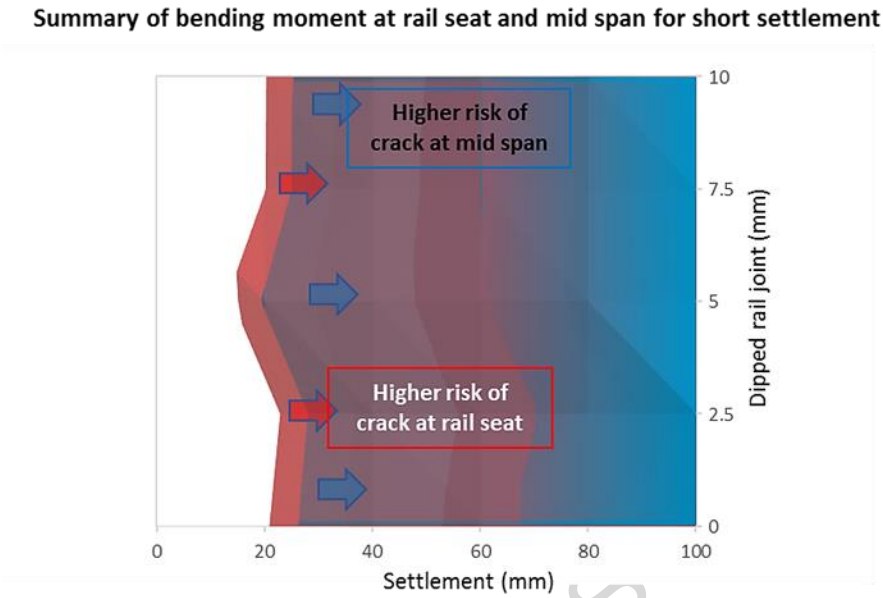

Fig. 26: Summary of bending moment at rail seat and midspan for short settlement

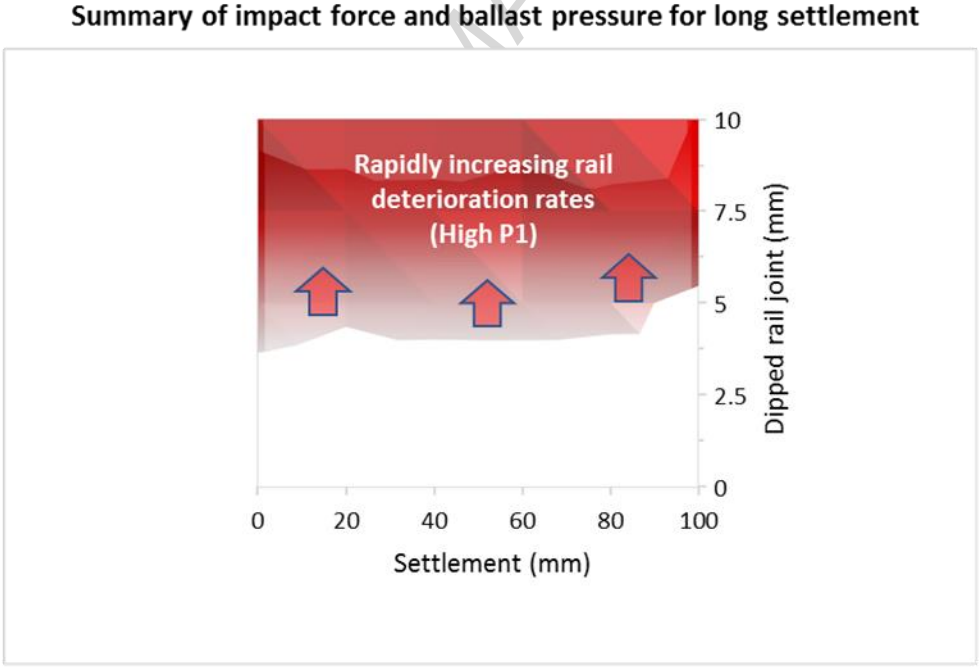

Fig. 27: Summary of wheel/rail interaction force and ballast pressure for long settlement

8. Final remarks

A numerical study was presented on the coupled influences between dipped rail joint and track settlement on dynamic loading conditions. To that aim, various models were used to simulate the effect caused by different amplitudes of rail joint and track settlement.

The results proposed that the development of a combination of dipped rail joint and differential track settlement lead to critical situations in cases of rail deterioration (due to excessive P1 force), track deterioration (due to excessive P2 force), beneath ballast component deterioration (over limit of ballast pressure), crack at rail head (high positive bending moment) and crack at mid span of sleeper (high negative bending moment). In general, the dynamic reaction increased with the amplitude of both dipped joint and track degradation, but it also depends on the specific point because some coupled profiles are able to decrease wheel/rail contact force. These insights will improve the efficiency of track and vehicle maintenance along with track design and the feasibility of railways as a viable means of transport.

Acknowledgements

The first author wishes to gratefully acknowledge the Australian Academy of Sciences (AAS) and Japan Society for Promotion of Science (JSPS) for his JSPS Invitation Research Fellowship (Long-term), Grant No L15701, at Track Dynamics Laboratory, Railway Technical Research Institute and at Concrete Laboratory, the University of Tokyo, Tokyo, Japan. The JSPS financially supports this work as part of the research project, entitled “Smart and reliable railway infrastructure”. The authors are very grateful to European Commission for H2020-MSCA-RISE

Project No. 691135 "RISEN: Rail Infrastructure Systems Engineering Network" (www.risen2rail.eu). We would like to acknowledge Australian RailCRC for educational version of D-Track and Jeff Leong (Currently at Network Rail) for benchmarking validation results. In addition, the sponsorships and assistance from CEMEX, Network Rail, and RSSB (Rail Safety and Standard Board, UK) are highly appreciated.

References

[1] C. Esveld, *Modern Railway Track*, The Netherlands MRT Press. (2001).

[2] B. Indraratna, C. Rujikiatkamjorn, and W. Salim, Advanced Rail Geotechnology – Ballasted Track, CRC Press, London, UK (2011).

[3] Kaewunruen S, Sussman JM and Matsumoto A (2016) Grand Challenges in Transportation and Transit Systems. Front. Built Environ. 2:4. doi: 10.3389/fbuil.2016.00004

[4] Dindar S., Kaewunruen S., An M., Sussman J.M. (2017) Bayesian Network-based probability analysis of train derailments caused by various extreme weather patterns on railway turnouts, Safety Science, in press. doi: 10.1016/j.ssci.2017.12.028

[5] Bin Osman M.H., Kaewunruen S., Jack A. (2017) Optimisation of schedules for the inspection of railway tracks, Proceedings of the Institution of Mechanical Engineers, Part F: Journal of Rail and Rapid Transit, in press. doi: 10.1177/0954409717721634

[6] Kaewunruen S. (2018) Monitoring of rail corrugation growth on sharp curves for track maintenance prioritization, International Journal of Acoustics and Vibration, 23(1), in press. doi: 10.20855/ijav.2018.23.11078

[7] Remennikov AM, Kaewunruen S. A review of loading conditions for railway track structures due to train and track vertical interaction. Struct Control Hlth 2008; 15(2):207-34.

[8] Kaewunruen S, Remennikov AM. Dynamic properties of railway track and its components: recent findings and future research direction. Insight Non Destr Test Cond Monit 2010; 52(1): 20-2.

[9] Dahlberg T. Railway track dynamics – a survey. Linköping: Linköping; University; 2003.

[10] Fry´ ba L. Vibration of solids and structures under moving loads. 3rd ed. Prague: Thomas Telford; 1999.

[11] Paixão, A., Fortunato, E., & Calçada, R., The effect of differential settlements on the dynamic response of the train–track system: A numerical study. *Engineering structures*, 216-224, 2015.

[12] Mandal, N. K., Dhanasekar, M., & Sun, Y. Q., Impact forces at dipped rail joints. *Proceedings of the Institution of Mechanical Engineers, Part F: Journal of Rail and Rapid Transit*, 271-282, 2014.

[13] Ishida M and Miura S (1992), Relationship between rail surface irregularity and dynamic wheel load, Proc. 10th Int. Wheelset Congress (Sydney), IEAust, pp.175‑179.

[14] Cai, Z. Modelling of rail track dynamics and wheel/rail interaction. PhD Theses, Queen's University, Canada, 1992.

[15] Iwnicki, S. Manchester Benchmarks for Rail Vehicle Simulation, Vehicle System Dynamics, 30 (3-4): 295-313, 1998.

[16] Steffens, D. M. Identification and development of a model of railway track dynamic behavior. MEng Thesis, Queensland University of Technology, Australia, 2005.

[17] Leong, J. Development of Limit State Design of Methodology for Railway Track. MEng Thesis, Queensland University of Technology, Australia, 2007.

[18] Tew G P, Marich S and Mutton P J, *A review of track design procedures, Vol 1: Rails*, Railways of Australia (ISBN 0 909582 02 5), 1991.

[19] Eisenmann, J., Germans gain a better understanding of track structure. *Railway Gazette International*, 305-310, 1972.

[20] Chandra, S., Rail joint and Welding of Rails. In S. Chandra, *Railway engineering* (pp. 294-337). New Delhi, India: Oxford university press, 2008.

[21] Jenkins., The effect of track and vehicle parameters on wheel/rail vertical dynamic force. Rail engineering Journal, 2-16, 1974.

[22] Paixão, A., Fortunato, E., & Calçada, R., The effect of differential settlements on the dynamic response of the train–track system: A numerical study. Engineering Structures, 216-224, 2015.

[23] Varandas, J. N., Hölscher, P., & Silva, M. A., Settlement of ballasted track under traffic loading: application to transition zones. Journal of Rail and Rapid Transit, Part F: Journal of Rail and Rapid Transit, 228(3), pp.242-259, 2014.

[24] Kaewunruen, S., Aikawa, A., Remennikov, A.M. (2017) Vibration attenuation at rail joints through under sleeper pads. Procedia Engineering, 189: 193-198. doi: 10.1016/j.proeng.2017.05.031

[25] Kaewunruen, S. and Remennikov, A.M., "Experimental determination of the effect of wet/dry ballast on dynamic sleeper/ballast interaction." ASTM J of Testing and Evaluation, 36(4): 412-415, 2008.

[26] Selig, E. T., & Waters, J. M., Track geotechnology and substructure management. Thomas Telford, London, 1994.

[27] Holtzendorff, K., & Gerstberger, U., Predicting Settlements of Ballasted Tracks due to Voided Sleepers. In Worl Congress Railway Research, Germany, 2001.

[28] Dahlberg, T., Railway track settlement - a literature review. Linkoping: Linkoping University, Sweden, 2003.

[29] Standards Australia, Australian Standard AS1085.14 Railway Track Materials, Part 14: Railway Prestressed Concrete Sleepers, Australia, 2003.

[30] Standards Australia, Australian Standard AS 7508. Track Forces and Stresses.

[31] RISSB; Rail industry safety and standards board, 2017

[32] Standards Australia, Australian Standard AS2758.7 Aggregates and Rock for Engineering Purposes - Railway Ballast, Australia, 1996.

[33] Wang, P., Design of high-speed railway turnouts: theory and applications. Academic Press, 2015.

[34] Kaewunruen S, Remennikov AM., (2008), Nonlinear transient analysis of a railway concrete sleeper in a track system, International Journal of Structural Stability and Dynamics 8 (03), 505-520.

[35] Kaewunruen S, Remennikov AM., (2008), Effect of a large asymmetrical wheel burden on flexural response and failure of railway concrete sleepers in track systems, Engineering Failure Analysis, 15 (8), 1065-1075.

[36] Remennikov AM., Kaewunruen S, (2008), Experimental load rating of aged railway concrete sleepers, Engineering Structures, 76, 147-162.

[37] Kaewunruen S, Remennikov AM., (2009), Structural safety of railway prestressed concrete sleepers, Australian Journal of Structural Engineering, 9 (2), 129-140.

[38] Ngamkhanong C, Li D, Remennikov AM, Kaewunruen S., Dynamic capacity reduction of railway prestressed concrete sleepers due to surface abrasions considering the effects of strain rate and prestressing losses, *International Journal of Structural Stability and Dynamics,* in press., 2018. doi: 10.1142/S0219455419400017

[39] Ishida M and Abe N (1993), Rail surface irregularity and bending fatigue of welded part, Proc 5th Int. Heavy Haul Railway Conf, Beijing, pp.302‑308.

[40] Chiengson, C. (2017) Coupled effects of dipped rails and track settlement on dynamic and impact loading conditions, MSc Thesis in Railway Systems Engineering and Integration, School of Engineering, The University of Birmingham, U.K. 120p.

[41] Kaewunruen, S., Lewandrowski, T., Chamniprasart, K. (2018) Dynamic responses of interspersed railway tracks to moving train loads, International Journal of Structural Stability and Dynamics 18 (01), 1850011. doi: 10.1142/S0219455418500116

[42] Mirza O, Kaewunruen S, Dinh C, Pervanic E., (2016) Numerical investigation into thermal load responses of railway transom bridge, Engineering Failure Analysis 60, 280-295. doi: 10.1016/j.engfailanal.2015.11.054

Highlights

- 440 multi-body simulations were carried out.
- It is the first to determine coupling train-track interaction over coupled short and long wavelength track defects for track maintenance prioritisation.
- Insights have been used to develop criteria for prioritising track inspection and maintenance.
- The understanding into failure mechanism of the coupling effects will help track engineers to better monitor and preventatively maintain ballasted track environments.